

# Phase field model for cell spreading dynamics

Mohammad Abu Hamed<sup>1,2</sup> and Alexander A. Nepomnyashchy<sup>1</sup>

<sup>1</sup>*Department of Mathematics, Technion - Israel Institute of Technology, Haifa 32000, Israel*

<sup>2</sup>*Department of Mathematics, The College of Sakhnin - Academic College for Teacher Education, Sakhnin 30810, Israel*

We suggest a 3D phase field model to describe 3D cell spreading on a flat substrate. The model is a simplified version of a minimal model that was developed in [1]. Our model couples the order parameter  $u$  with 3D polarization (orientation) vector field  $\mathbf{P}$  of the actin network. We derive a closed integro-differential equation governing the 3D cell spreading dynamics on a flat substrate, which includes the normal velocity of the membrane, curvature, volume relaxation rate, a function determined by the molecular effects of the subcell level, and the adhesion effect. This equation is easily solved numerically. The results are in agreement with the early fast phase observed experimentally in [2]. Also we find agreement with the universal power law [3] which suggest that cell adhesion or contact area versus time behave as  $\sim t^{1/2}$  in the early stage of cell spreading dynamics, and slow down at the next stages.

## I. INTRODUCTION

Understanding the phenomenon of cell spreading has numerous potential applications, which include designing biomaterials for optimal control of cell behavior [4], insight into cell morphology [5], and developing efficient methods for gene transfection in biomaterials [6].

In the last two decades, several models have been developed that describe cell spreading on a flat substrate. Those models take into account the elastic [7], [8] or visco-elastic properties of the cell and/or the substrate [4], [9]. In addition, those models describe the dynamics of some subcellular components such as cortical cytoskeleton, cell nuclear, actin filaments, and microtubules [10], [11]. Also, they consider the mechanical interactions between cell adhesion molecules like cross-membrane protein, molecular clutches, and the extracellular property of the substrate. There exist other models that describe cell spreading on non-flat substrate such as V or Y-shaped micro-patterned substrates [12]. All of the previous models were compared with and validated by experimental measurements.

Typically, the implementation of computational models needs hard numerical simulations based on finite elements methods [11], [13] or minimizing some free energy functionals [10]; some models include stochastic effects [12].

Based on experimental data and measurements, some universality property of cell spreading have been discovered. Usually early spreading is isotropic. Cell spreading may experience three sequential phases, basal (cell touches the substrate), fast continuous spreading (generation of lamellipodial sheet), and periodic local contractile spreading [2]. These phases obey a power-law area growth with distinct exponents when we plot cell adhesion area (contact area) versus time. Later the authors in [3] succeed to explain these power-law relationships with a relatively simple physical model. They consider energy balance and assume that actin cortex is a viscous liquid [14].

A minimal computational phase field model of 3D cell

crawling on general substrate topography was developed in [1]. In the present paper we consider a simplified version of that model. We choose the substrate to be a flat surface,  $z = 0$ , in order to model the dynamics of cell spreading on the plane. Unlike the models mentioned above, our model is simple. We describe the cell spreading dynamics by a single scalar non-local partial differential equation of the cell interface (16), which could be solved easily with Wolfram Mathematica program. Our model is in qualitative agreement with observations at the early fast phase, and the universal power law at the earlier stages of cell spreading.

The structure of the paper is as follows. In Sec. II we present the minimal 3D phase field model. In Sec. III we introduce the proper length and time scales of the spreading dynamics. We perform asymptotic analysis and find the fields at the leading order, and then we use the solvability condition to derive a closed evolutionary nonlocal equation that describes the cell interface dynamics (16). We solve this equation numerically via the function `NDSolve` of Wolfram Mathematica. We reveal the agreement with the universal power law. Finally, in Sec. IV we present the conclusions.

## II. FORMULATION OF THE PROBLEM

In order to describe the dynamics of cell located in region  $z > 0$  and spreading on the flat substrate  $z = 0$ , see Fig. 1, we extend the problem into the whole space, postulating the reflection symmetry or antisymmetry of our fields under the transformation  $z \rightarrow -z$ .

Let us consider the following simplified version of the

model that was formulated in [1]:

$$u_t = D_u \nabla^2 u - (1 - u)(\delta - u)u - \alpha \nabla u \cdot \mathbf{P} - k \nabla \Psi_u \cdot \nabla u, \quad (1a)$$

$$\delta = \frac{1}{2} + \mu \delta V - \sigma |\mathbf{P}|^2, \quad \delta V(t) = \int u d^3 r - v_0, \quad (1b)$$

$$\mathbf{P}_t = D_p \nabla^2 \mathbf{P} - \tau^{-1} \mathbf{P} - \beta \Psi_p(z) \left[ (1 - \nu) \hat{P} \nabla u + \nu \nabla u \right], \quad (1c)$$

$$u(r=0) = 1, \quad u(r \rightarrow \infty) = 0, \quad (1d)$$

$$\mathbf{P}(r=0) = \mathbf{P}(r \rightarrow \infty) = 0; \quad (1e)$$

see Fig. 1; here  $u$  is the order parameter that is close to 1 inside the cell and 0 outside, and  $\mathbf{P}$  is the three-dimensional polarization vector field representing the actin orientations. In (1c),  $\hat{P} = \hat{I} - \hat{n}\hat{n}$  is the projection operator onto the local tangential plane, where  $\hat{n} = \nabla \Psi_p / |\nabla \Psi_p|$  (in our case  $\hat{n} = \pm \hat{z}$ ). Therefore,

$$\hat{P} \nabla u = \nabla u - \hat{z} \hat{z} \cdot \nabla u = u_x \hat{x} + u_y \hat{y}.$$

The parameter  $0 \leq \nu \leq 1$  model the contribution of actin polarization from the tangential limit  $\nu = 0$ , and the isotropic limit  $\nu = 1$ .

The constant parameters of the problem are:  $D_u$  is the stiffness of diffuse interface,  $D_p$  is the diffusion coefficient for  $\mathbf{P}$ ,  $\alpha$  is the coefficient characterizing advection of  $u$  by  $\mathbf{P}$ ,  $\beta$  determines the creation of  $\mathbf{P}$  at the interface,  $\tau^{-1}$  is the inverse time of the degradation of  $\mathbf{P}$  inside the cell,  $v_0$  is twice the overall initial volume of the cell due to the reflection symmetry,  $\mu$  is the stiffness of the volume constraint, and  $\sigma$  is the contractility of actin filament bundles. All the parameters listed above are positive.

In addition, we make the basic assumption that the ratio  $\epsilon$  of the thickness of the cell wall (i.e., the width of the transition zone, where  $u$  is changed from nearly 1 to nearly 0) to the characteristic size of the cell is small,  $\epsilon \ll 1$ , see Fig. 1. Motivated by [1], we define the static fields as

$$\Psi_u(z) = e^{-(\epsilon z)^2 / D_u}, \quad \Psi_p(z) = e^{-(\epsilon z)^2 / l_p}, \quad l_p = \tau D_p, \quad (2)$$

see Fig. 2. We choose  $l_p > D_u$  to allow more substantial actin inside the cell. The appearance of  $\epsilon$  in the exponents of (2) allows to avoid boundary layer problem complications both in time and space. The expression  $k \nabla \Psi_u \cdot \nabla u$  in (1a) models the adhesion effect of the substrate;  $k$  is adhesion strength parameter. Notice that  $\nabla \Psi_u \cdot \nabla u = O(1)$  only in region nearby the substrate and also at the cell boundary or membrane i.e., where protrusion holds. Also the appearance of  $\Psi_p \nabla u$  in (1c) allows high actin concentration nearby the flat substrate  $z = 0$  where protrusions are developed during cell spreading, and low actin concentration otherwise, see Fig. 1. This scenario is in agreement with experimental studies, see [15], [7], and the review paper [16].

We apply the spherical coordinate system, see Fig. 1, hence  $u = u(r, \theta, \varphi, t)$ ,  $\mathbf{P}(r, \theta, \varphi, t) = p\hat{r} + q\hat{\theta} + w\hat{\varphi}$ . We define the iso-surface of the interface as  $u(r = \rho(\theta, \varphi, t)) =$

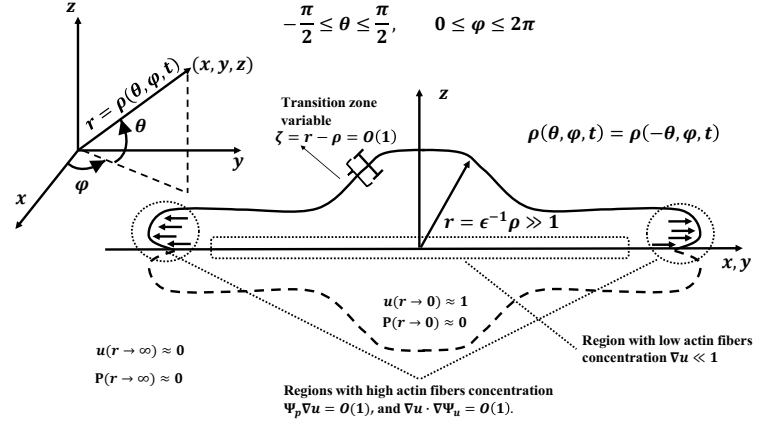


FIG. 1. A schematic description of cell spreading dynamics in spherical coordinate system, and the boundary conditions of the simplified model (1). The cell is only the shape in the upper region  $z \geq 0$  while the model (1) is formulated in the hole space with reflection symmetry assumption with respect of the substrate plane  $z = 0$ , (4). The thickness of the cell wall (i.e., the width of the transition zone, where  $u(r, t)$  is changed from nearly 1 to nearly 0) is  $O(1)$ , and the cell size is large. Therefore the ratio  $\epsilon$  of the thickness of the cell wall to the size of the cell is small. In addition we emphasize the regions where the fields  $\nabla \Psi_u \cdot \nabla u$ , and  $\Psi_p \nabla u$  give their main contribution and exponentially small otherwise. These are the regions where protrusions developed.

1/2. As a result of our definition of the spherical coordinate, we have

$$(r, \theta, \varphi), \quad 0 < r < \infty, \quad -\frac{\pi}{2} < \theta < \frac{\pi}{2}, \quad 0 < \varphi < 2\pi, \quad (3a)$$

$$x = r \cos \theta \cos \varphi, \quad y = r \cos \theta \sin \varphi, \quad z = r \sin \theta, \quad (3b)$$

$$\nabla = \hat{r} \partial_r + \hat{\theta} \frac{\partial}{r} + \hat{\varphi} \frac{\partial}{r \cos \theta}, \quad (3c)$$

$$\nabla^2 = \partial_r^2 + \frac{2\partial_r}{r} + \frac{1}{r^2} \left( \partial_\theta^2 - \tan \theta \partial_\theta + \frac{\partial_\varphi^2}{\cos^2 \theta} \right), \quad (3d)$$

$$\nabla^2 \mathbf{P} = \hat{r} \nabla^2 p + \hat{\theta} \nabla^2 q + \hat{\varphi} \nabla^2 w + O\left(\frac{1}{r^2}\right). \quad (3e)$$

One can calculate,

$$\begin{aligned} & \left[ (1 - \nu) \hat{P} + \nu \hat{I} \right] \nabla u = u_x \hat{x} + u_y \hat{y} + \nu u_z \hat{z} = \nabla u + (\nu - 1) u_z \hat{z} \\ & = \left[ (1 + (\nu - 1) \sin^2 \theta) u_r + (\nu - 1) \frac{\sin 2\theta}{2r} u_\theta \right] \hat{r} + \\ & \left[ (1 + (\nu - 1) \cos^2 \theta) \frac{u_\theta}{r} + (\nu - 1) \frac{\sin 2\theta}{2} u_r \right] \hat{\theta} + \frac{u_\varphi}{r \cos \theta} \hat{\varphi}. \end{aligned}$$

Notice that due to the appearance of  $\Psi_{u,p}(z)$ , the system (1a)-(1e) does not have any rotationally spherical symmetric solutions. Therefore, we have to look for general shape solutions.

The reflection symmetry assumption relative to the substrate plane  $z = 0$ , yields the conditions,

$$u(-\theta) = u(\theta), \quad \rho(-\theta) = \rho(\theta), \quad (4a)$$

$$p(-\theta) = p(\theta), \quad w(-\theta) = w(\theta), \quad q(-\theta) = -q(\theta) \quad (4b)$$

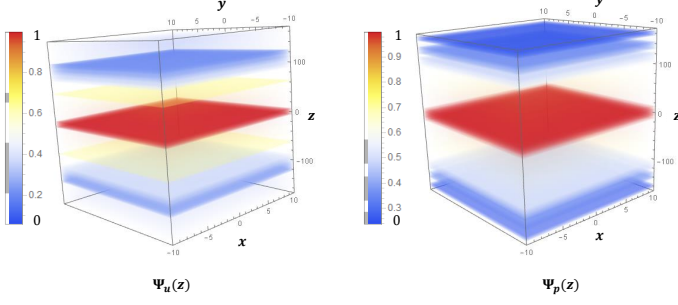


FIG. 2. Plot of the density functions  $\Psi_{u,p}$  in (2). Notice that  $\Psi_{u,p} = O(1)$  nearby the substrate  $z = 0$  (red region) while attenuate far away (blue region). The width of the layer where  $\Psi_p = O(1)$  is  $O(\sqrt{\tau D_p})$ . Therefore it is thicker than layer where  $\Psi_u = O(1)$  that is  $O(\sqrt{D_u})$ .

### III. DYNAMICS OF GENERAL SHAPE INTERFACE

In order to balance the front dynamics with curvature we impose the following scaling that describes slow dynamics of a large-size cell [17],

$$\tilde{t} = \epsilon^2 t, \quad \rho(\theta, \varphi, t) = \epsilon^{-1} R(\theta, \varphi, t), \quad \epsilon \ll 1. \quad (5)$$

The transition zone variable is defined as

$$\zeta = r - \rho(\theta, \varphi, t) = O(1). \quad (6)$$

Also we define,

$$R(\theta, \varphi, t) = \tilde{R}(\theta, \varphi, \tilde{t}), \quad u(r, \theta, \varphi, t) = \tilde{u}(\zeta, \theta, \varphi, \tilde{t}), \quad (7a)$$

$$\mathbf{P}(r, \theta, \varphi, t) = \tilde{\mathbf{P}}(\zeta, \theta, \varphi, \tilde{t}). \quad (7b)$$

The chain rule yields

$$\partial_t = -\epsilon \tilde{R}_{\tilde{t}} \partial_{\zeta} + \epsilon^2 \partial_{\tilde{t}}, \quad \partial_r = \partial_{\zeta}. \quad (8)$$

later on we drop the tildes. It holds that

$$\frac{1}{r} = \frac{\epsilon}{R} - \frac{\epsilon^2 \zeta}{R^2} + \dots, \quad (9a)$$

$$\Psi_p(z) = e^{-(\epsilon z)^2 / l_p} = e^{-\epsilon^2 r^2 \sin^2 \theta / l_p} = e^{-\epsilon^2 (\zeta + \epsilon^{-1} R)^2 \sin^2 \theta / l_p} \sim e^{-R^2 \sin^2 \theta / l_p}, \quad (9b)$$

$$\nabla \Psi_u \sim \frac{-\epsilon R}{D_u} e^{-R^2 \sin^2 \theta / D_u} \left( 2 \sin^2 \theta \hat{r} + \sin 2\theta \hat{\theta} \right). \quad (9c)$$

In addition one can calculate,

$$\partial_\theta = -\epsilon^{-1} R_\theta \partial_\zeta + \partial_\theta, \quad \partial_\varphi = -\epsilon^{-1} R_\varphi \partial_\zeta + \partial_\varphi, \quad (10a)$$

$$\partial_\theta^2 = \epsilon^{-2} R_\theta^2 \partial_\zeta^2 - \epsilon^{-1} (R_{\theta\theta} \partial_\zeta + 2R_\theta \partial_\zeta^2 \theta) + \partial_\theta^2, \quad (10b)$$

$$\partial_\varphi^2 = \epsilon^{-2} R_\varphi^2 \partial_\zeta^2 - \epsilon^{-1} (R_{\varphi\varphi} \partial_\zeta + 2R_\varphi \partial_\zeta^2 \varphi) + \partial_\varphi^2, \quad (10c)$$

$$\frac{\partial_\theta}{r} = -\frac{R_\theta}{R} \partial_\zeta + O(\epsilon), \quad \frac{\partial_\theta}{r^2} = -\epsilon \frac{R_\theta}{R^2} \partial_\zeta + O(\epsilon^2), \quad (10d)$$

$$\frac{\partial_\varphi}{r} = -\frac{R_\varphi}{R} \partial_\zeta + O(\epsilon), \quad \frac{\partial_\varphi}{r^2} = -\epsilon \frac{R_\varphi}{R^2} \partial_\zeta + O(\epsilon^2), \quad (10e)$$

$$\begin{aligned} \nabla^2 u &= \left( 1 + \frac{R_\theta^2}{R^2} + \frac{R_\varphi^2}{R^2 \cos^2 \theta} \right) u_{\zeta\zeta} + \\ &\epsilon \left[ \left( \frac{2}{R} + \frac{R_\theta}{R^2} \tan \theta - \frac{R_{\theta\theta}}{R^2} - \frac{R_{\varphi\varphi}}{R^2 \cos^2 \theta} \right) u_\zeta \right. \\ &\quad \left. - \frac{2}{R^2} \left( R_\theta u_{\zeta\theta} + \frac{R_\varphi}{\cos^2 \theta} u_{\zeta\varphi} \right) \right. \\ &\quad \left. - \frac{2\zeta}{R^3} \left( R_\theta^2 + \frac{R_\varphi^2}{\cos^2 \theta} \right) u_{\zeta\zeta} \right] + O(\epsilon^2). \end{aligned} \quad (10f)$$

We can approximate the nonlocality in (1b) as follows,

$$\int u d^3 r \sim \frac{\epsilon^{-3}}{3} \int_0^{2\pi} d\varphi \int_{-\pi/2}^{\pi/2} R^3(\theta, \varphi, t) \cos \theta d\theta. \quad (11)$$

Consider the following scaling of the model parameters

$$\alpha = \epsilon A, \quad \frac{4\pi\mu}{3} \epsilon^{-3} = \epsilon M, \quad \sigma = \epsilon S, \quad v_0 = \epsilon^{-3} V_0, \quad k = O(1). \quad (12)$$

Let us introduce the expansions

$$u = u_0 + \epsilon u_1 + \dots, \quad p = p_0 + \epsilon p_1 + \dots \quad (13)$$

We define the auxiliary function ,

$$\Lambda(\theta, \varphi, t) = \left( 1 + \frac{R_\theta^2}{R^2} + \frac{R_\varphi^2}{R^2 \cos^2 \theta} \right)^{-1/2},$$

and the function,

$$\begin{aligned} \Phi(\tau, D_u, D_p, \zeta) &= \\ &\frac{1}{8} \sqrt{\frac{\tau}{2D_u D_p}} \int_{-\infty}^{\infty} e^{-|s|/\sqrt{\tau D_p}} \cosh^{-2} \left( \frac{s - \zeta}{\sqrt{8D_u}} \right) ds, \end{aligned}$$

that are basic for our next analysis.

We substitute the length, time (5), and the parameters scaling (12) into system (1). We write the system (1) in the transition zone variable (6)-(7) via the expansions and the chain rules (8)-(11). We substitute the asymptotic expansions (13) and finally we collect terms of the same order.

Consequently we obtain at the leading order the fol-

lowing system,

$$\begin{aligned}
D_u \Lambda^{-2} u_{0\zeta} &= (1 - u_0) \left( \frac{1}{2} - u_0 \right) u_0, \\
D_p \Lambda^{-2} p_{0\zeta} - \tau^{-1} p_0 &= \\
\beta e^{-R^2 \sin^2 \theta / l_p} &\left[ 1 + (\nu - 1) \sin^2 \theta - (\nu - 1) \frac{\sin 2\theta}{2} \frac{R_\theta}{R} \right] u_{0\zeta}, \\
D_p \Lambda^{-2} q_{0\zeta} - \tau^{-1} q_0 &= \\
-\beta e^{-R^2 \sin^2 \theta / l_p} &\left[ (1 + (\nu - 1) \cos^2 \theta) \frac{R_\theta}{R} - (\nu - 1) \frac{\sin 2\theta}{2} \right] u_{0\zeta}, \\
D_p \Lambda^{-2} w_{0\zeta} - \tau^{-1} w_0 &= -\beta e^{-R^2 \sin^2 \theta / l_p} \frac{R_\varphi}{R \cos \theta} u_{0\zeta}.
\end{aligned}$$

Following the Ginzburg-Landau theory and Fourier transform method the solution of this system is given by,

$$\begin{aligned}
u_0(\zeta) &= \frac{1}{2} \left[ 1 - \tanh \left( \frac{\Lambda \zeta}{\sqrt{8D_u}} \right) \right], \\
p_0(\zeta) &= \beta \lambda_p \Lambda \Phi(\Lambda \zeta), \\
\lambda_q &= e^{-R^2 \sin^2 \theta / l_p} \left[ 1 + (\nu - 1) \sin^2 \theta - (\nu - 1) \frac{\sin 2\theta}{2} \frac{R_\theta}{R} \right], \\
q_0(\zeta) &= -\beta \lambda_q \Lambda \Phi(\Lambda \zeta), \\
\lambda_q &= e^{-R^2 \sin^2 \theta / l_p} \left[ (1 + (\nu - 1) \cos^2 \theta) \frac{R_\theta}{R} - (\nu - 1) \frac{\sin 2\theta}{2} \right], \\
w_0(\zeta) &= -\beta \lambda_w \Lambda \Phi(\Lambda \zeta), \\
\lambda_w &= e^{-R^2 \sin^2 \theta / l_p} \frac{R_\varphi}{R \cos \theta}.
\end{aligned}$$

Notice that these results satisfy the symmetry conditions (4), if  $R(-\theta) = R(\theta)$ .

The equation for the correction term  $u_1$  at the order  $O(\epsilon)$  have the form,

$$L[u_1] = \text{RHS}, \quad (15)$$

$$L = D_u \Lambda^{-2} \partial_\zeta^2 - \left( \frac{1}{2} - 3u_0 + 3u_0^2 \right) \hat{I},$$

$$\text{RHS} = -R_t u_{0\zeta} -$$

$$D_u \left[ \left( \frac{2}{R} + \frac{R_\theta}{R^2} \tan \theta - \frac{R_{\theta\theta}}{R^2} - \frac{R_{\varphi\varphi}}{R^2 \cos^2 \theta} \right) u_{0\zeta} \right.$$

$$- \frac{2}{R^2} \left( R_\theta u_{0\zeta\theta} + \frac{R_\varphi}{\cos^2 \theta} u_{0\zeta\varphi} \right)$$

$$\left. - \frac{2\zeta}{R^3} \left( R_\theta^2 + \frac{R_\varphi^2}{\cos^2 \theta} \right) u_{0\zeta\zeta} \right]$$

$$+ A \left( p_0 - \frac{R_\theta}{R} q_0 - \frac{R_\varphi}{R \cos \theta} w_0 \right) u_{0\zeta}$$

$$- \frac{k}{D_u} R \cdot e^{-R^2 \sin^2 \theta / D_u} \left( 2 \sin^2 \theta - \sin(2\theta) \frac{R_\theta}{R} \right) u_{0\zeta} +$$

$$(1 - u_0) u_0 \left\{ \tilde{V}(t) - S(p_0^2 + q_0^2 + w_0^2) \right\},$$

where the volume variation have the form,

$$\tilde{V}(t) = M \left[ \frac{1}{4\pi} \int_0^{2\pi} d\varphi \int_{-\pi/2}^{\pi/2} R^3(\theta, \varphi, t) \cos \theta d\theta - \frac{3}{4\pi} V_0 \right].$$

We apply the solvability condition, which is the orthogonality of the right-hand side (RHS) of equation (15) to the solution  $u_{0\zeta}$  of the homogenous equation  $L[u] = 0$  of (15) i.e.,

$$\int_{-\infty}^{\infty} \text{RHS}(\zeta) \cdot u_{0\zeta}(\zeta) d\zeta = 0.$$

We therefore obtain a closed equation governing the interface dynamics  $R(\theta, \varphi, t)$ ,

$$a \Lambda R_t = -2a D_u \mathcal{H} - \tilde{V} + \Omega - N, \quad (16)$$

where

$$\mathcal{H} = \frac{1}{2} \nabla \cdot \hat{n} = \frac{1}{2} \nabla \cdot \left( \frac{\nabla(r - R)}{|\nabla(r - R)|} \right) \quad (17)$$

is the mean local curvature of the surface  $r = R(\theta, \varphi, t)$ , see Appendix A, and

$$\begin{aligned}
\Omega(\theta, \varphi, t) &= 6\beta A \Omega_1 \Lambda^2 \left( \lambda_p + \frac{R_\theta}{R} \lambda_q + \frac{R_\varphi}{R \cos \theta} \lambda_w \right) + \\
&6\beta^2 S \Omega_2 \Lambda^2 (\lambda_p^2 + \lambda_q^2 + \lambda_w^2),
\end{aligned}$$

$$\Omega_1(\tau, D_u, D_p) = \int_{-\infty}^{\infty} \Phi(\xi) \bar{u}_0^2(\xi) d\xi,$$

$$\Omega_2(\tau, D_u, D_p) =$$

$$\int_{-\infty}^{\infty} \Phi^2(\xi) (\bar{u}_0(\xi) - 1) \bar{u}_0(\xi) \bar{u}_{0\xi}(\xi) d\xi > 0,$$

where

$$\bar{u}_0(\xi) = \frac{1}{2} \left[ 1 - \tanh \left( \frac{\xi}{\sqrt{8D_u}} \right) \right].$$

The adhesion effect is implemented by

$$N = \frac{ak}{D_u} \Lambda R \cdot e^{-R^2 \sin^2 \theta / D_u} \left( 2 \sin^2 \theta - \sin(2\theta) \frac{R_\theta}{R} \right)$$

For more details and explanations about arguments for the derivation of the governing equation (16) see [18], [17], and [19].

Equation (16) comes in conjunction with the Neumann boundary conditions

$$R_\theta(\theta = 0) = R_\theta(\theta = \pi/2) = 0, \quad (18)$$

and some initial interface  $R(t = 0)$ .

In order to model cell spreading, we may consider the axi-symmetric case  $R_\varphi = 0$ , since according to experimental observation, the onset of cell spreading is isotropic [2]. As for the initial interface shape, we take the truncated sphere with radius  $R_0$  and center  $(0, 0, \eta)$ , see Fig. 3(a).

$$R(t = 0) = \eta \sin \theta + \sqrt{R_0^2 - \eta^2 \cos^2 \theta}, \quad 0 \leq \eta \leq 1. \quad (19)$$

Then the initial normalized volume in this case is given by

$$V_0 = \int_0^{\pi/2} R(t=0)^3 \cos \theta d\theta,$$

which is twice the volume of the truncated sphere.

In Fig. 3(a)-(f) we present the sequence of plots that show the results of the numerical simulation of the interface  $R(\theta, \varphi, t)$  according to equation (16) and boundary condition (18). We use the function `NDSolve` of Wolfram Mathematica. We plot  $R(\theta, \varphi, t)$  only in the upper region  $0 \leq \theta \leq \pi/2$ , the plot in the lower region is only a mirror reflection of the upper surface due to our symmetry assumption (4). Following experimental scenarios where the spherical-like cell almost touch the substrate we may take the parameters of our initial interface as  $\eta = 0.95$ , and  $R_0 = 1$ , see Fig. 3(a). This simulation as we see describes cell spreading. We begin from almost full sphere and end up with ellipsoid-like shape which is the steady state solution of the system (16), (18), and (19). In Fig. 3(g) we display the cell height  $R(\pi/2, t)$  which decreases from almost 2 to 1.21, while in Fig. 3(h) we display the cell contact area (radius)  $R(0, t)$  which increases to 2.

In addition Fig. 3(g)-(h) display the fast spreading phenomena at the beginning of cell spreading in agreement with the continuous spreading fast phase that was observed experimentally in [2]. Also, in Fig 3(i) we consider the Log-Log plot of the cell radius versus time, also we plot the piecewise function that connect two function of the form  $b_1 t^{1/2}$ , and  $b_2 t^{1/4}$ , for a proper choice of the parameters  $b_{1,2}$ , and for the connecting point. We notice the agreement with the universal power law [3] that suggest that cell adhesion or contact area versus time behave as  $\sim t^{1/2}$  in the early state of cell spreading dynamics, and slow down in the next states. The plot of the slope  $\sim t^{1/4}$  in Fig. 3(i) is only to emphasize the slowing down of the next phase.

In Fig. 4 we perform similar analysis where we choose  $D_u = 0.5$ , and  $D_p = 0.02$  while the other parameters remain as those of Fig. 3. Notice that in this case we have  $\tau D_p < D_u$ , unlike the previous case of Fig. 3

#### IV. CONCLUSION

We utilize a simplified version of minimal 3D phase field model that was developed in [1], in order to model cell spreading dynamics on a flat substrate. The model (1) couples the order parameter  $u$  with 3D polarization (orientation) vector field  $\mathbf{P}$  of the actin network. The model is formulated in the whole space but with appropriate symmetry conditions with respect to transformation  $z \rightarrow -z$ , (4).

After we introduce the proper time and length scale and perform asymptotic expansion, we solve equations for the fields at the leading order. As a result of the solvability condition we derive a closed integro-differential

equation (16) governing the 3D cell spreading dynamics, which includes the normal velocity  $\omega_n = \Lambda R_t$  of the membrane, curvature  $\mathcal{H}$ , volume relaxation rate  $\tilde{V}$ , a function  $\Omega(t)$  determined by the molecular effects of the subcell level, and the adhesion effect  $N$ .

Excluding the adhesion effect this result is similar to the 2D case which describe the onset of 2D cell dynamics on flat substrate [17] and 3D case that describe the onset of 3D cell motility immersed in 3D extracellular matrices [19].

The equation governing the interface or membrane dynamics during spreading may be presented in the form:

$$\omega_n = -2D_u \mathcal{H} - \tilde{V} + \Omega - N,$$

after we put the proper scaling transformation,  $t \rightarrow a^2 t$  and  $R(t) \rightarrow aR(t)$  in (16). This equation is easily solved numerically via the function `NDSolve` of Wolfram Mathematica. The simulation present cell spreading with significant high decreasing and radius increasing of the initial truncated spheres, see Fig 3, Fig. 4

These results are in agreement with the early fast phase that was observed experimentally in [2]. Surprisingly, the result are in qualitative agreement with universal power law which suggest that adhesion or contact area versus time behave as  $\sim t^{1/2}$  in the early state of cell spreading dynamics, and then it slow down. The appearance of the slope  $\sim t^{1/4}$  in Fig. 3(i) is only to emphasize the slowing down of the later phase. This is a surprising result since in our phase field model we did not assume any viscosity property of the cell membrane as it is assumed in [3].

#### Appendix A

Here we give an explicit expression for the mean curvature of a surface given in spherical coordinate description  $r = R(\theta, \varphi, t)$ , see Fig. 1. Following the definition (17),(3), one can calculate,

$$\begin{aligned} \nabla \cdot \hat{n} = \Lambda & \left\{ \frac{2}{R} - \frac{R_{\theta\theta}}{R^2} + \frac{R_\theta \tan \theta}{R^2} - \frac{R_{\varphi\varphi}}{R^2 \cos^2 \theta} \right\} \\ & + \Lambda^3 \left\{ \frac{1}{R^3} \left( R_\theta^2 + \frac{R_\varphi^2}{\cos^2 \theta} \right) + \frac{R_\theta^2 R_{\theta\theta}}{R^4} + \frac{2R_\theta R_\varphi R_{\theta\varphi}}{R^4 \cos^2 \theta} \right. \\ & \left. + \frac{R_\varphi^2}{R^4 \cos^4 \theta} \left( \frac{1}{2} R_\theta \sin 2\theta + R_{\varphi\varphi} \right) \right\} \end{aligned} \quad (\text{A1})$$

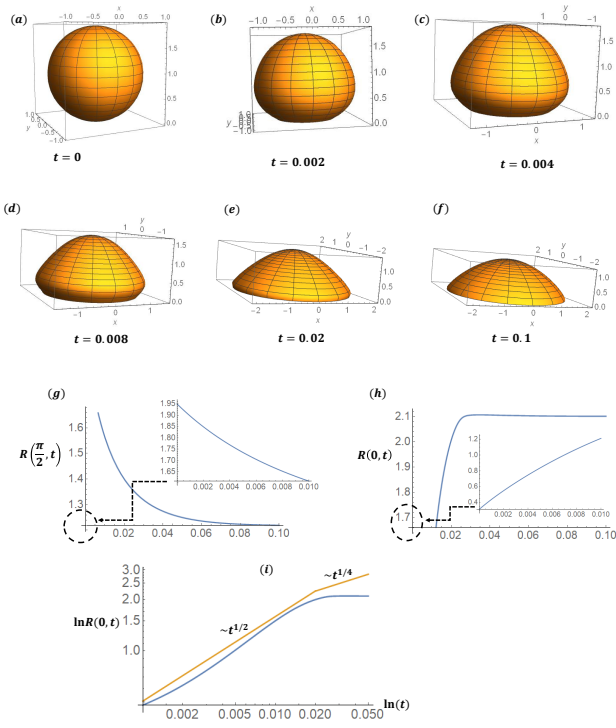


FIG. 3. (a)-(f) Time sequence of the simulation of the axisymmetric case of equation (16) with initial upwards shifted sphere (19) with radius  $R_0 = 1$  and center  $(0, 0, 0.95)$ . We employ the following value of parameters  $\beta = 5, A = 1, \tau = 10, D_u = 1, D_p = 0.2, M = 8, S = 2, \nu = 0.5, k = 15$ . (g) is the plot of the ellipsoid like height  $R(\pi/2, t)$ , (h) is the plot of the ellipsoid like radius  $R(0, t)$ , both in the time interval  $0 \leq t \leq 0.1$ . Notice the stationary ellipsoid-like has height 1.21 and radii 2. (i) Log-Log plot of the cell radius  $R(0, t)$  versus time  $t$ . Also we plot the piecewise function that connect two function of the form  $b_1 t^{1/2}$ , and  $b_2 t^{1/4}$ , for a proper choice of the parameters  $b_{1,2}$ , and for the connecting point. Notice the qualitative agreement with the universal power law in the initial fast phase and next the slower phase. The appearance of the slope  $\sim t^{1/4}$  in (i), is shown only to emphasize the slowing down of the later phase.

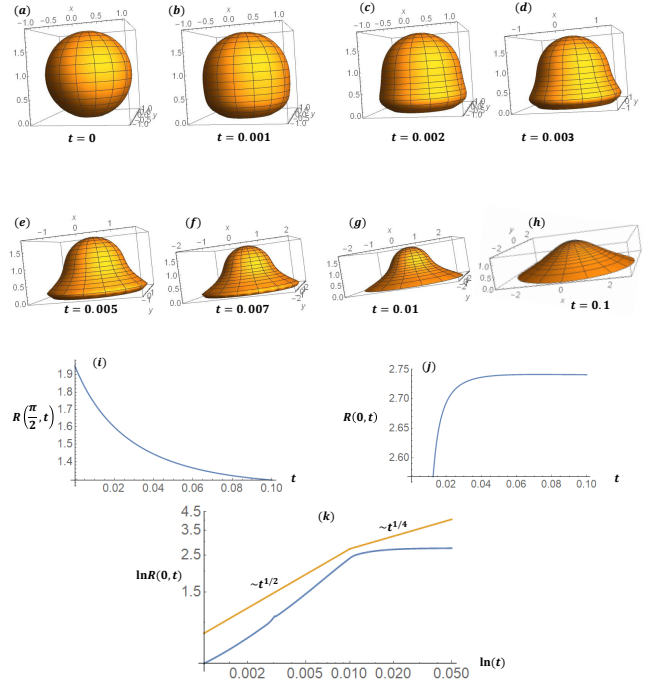


FIG. 4. (a)-(h) Time sequence of the simulation of the axisymmetric case of equation (16). We employ following value of parameters  $D_u = 0.5, D_p = 0.02$ , the other parameters and the initial sphere are as in Fig 3. (i) is the plot of the ellipsoid like height  $R(\pi/2, t)$ , (j) is the plot of the ellipsoid like radius  $R(0, t)$ , both in the time interval  $0 \leq t \leq 0.1$ . Notice the stationary ellipsoid-like has height 1.3 and radii 2.74. Notice that here we have  $\tau D_p < D_u$ , unlike the previous case of Fig. 3. (k) Log-Log plot as that of Fig. 3.

- 
- [1] B. Winkler, I. S. Aranson, and F. Ziebert, “Confinement and substrate topography control cell migration in a 3d computational model,” *Communications Physics* **2:82** (2019).
- [2] Dobereiner, Dubin-Thaler, Giannone, Xenias, and Sheetz, “Dynamic phase transitions in cell spreading,” *Physical review letters* **93** (2004).
- [3] Cuvelier, Thery, Chu, Dufour, Thiery, Bornens, Nassoy, and Mahadevan, “The universal dynamics of cell spreading,” *Current Biology* **17**, 694699 (2007).
- [4] Z. Gong, S. E. Szczesny, S. R. Caliarie, E. E. Charrier, O. Chaudhuri, X. Cao, Y. Lin, R. L. Mauck, P. A. Janmey, J. A. Burdick, and V. B. Shenoy, “Matching material and cellular timescales maximizes cell spreading on viscoelastic substrates,” *PNAS* **115 (12)**, E2686–E2695 (2018).
- [5] J. Folkman and A. Moscona, “Role of cell shape in growth control,” *Nature* **273**, 345349 (1978).
- [6] Y. Yang, X. Wang, X. Hu, N. Kawazoe, Y. Yang, and G. Chen, “Influence of cell morphology on mesenchymal stem cell transfection,” *ACS Appl. Mater. Interfaces* **11**, 1932–1941 (2019).
- [7] Y. Li, D. Lovett, Q. Zhang, S. Neelam, R. A. Kuchibhotla, R. Zhu, G. G. Gundersen, T. P. Lele, and R. B. Dickinson, “Moving cell boundaries drive nuclear shaping during cell spreading,” *Biophysical Journal* **109** (2015).
- [8] Y. Xiong, P. Rangamani, M. A. Fardin, A. Lipshtat, B. D. Thaler, O. Rossier, M. P. Sheetz, and R. Iyengar, “Mechanisms controlling cell size and shape during isotropic cell spreading,” *Biophysical Journal* **98**, 21362146 (2010).
- [9] N. Nisenholz, K. Rajendran, Q. Dang, H. Chen, R. Kemkemer, R. Krishnan, and A. Zemel, “Active mechanics and dynamics of cell spreading on elastic substrates,” *Soft Matter* **10** (2014).
- [10] Y. Fang and K. W. C. Lai, “Modeling the mechanics of cells in the cell–spreading process driven by traction forces,” *Physical Review E* **93** (2016).
- [11] F. J. Vernerey and M. Farsad, “A mathematical model of the coupled mechanisms of cell adhesion, contraction and spreading,” *J Math Biol* **68(4)**, 9891022 (2014).
- [12] E. McEvoy, V. S. Deshpande, and P. McGarry, “Free energy analysis of cell spreading,” *Journal of the Mechanical Behavior of Biomedical Materials* **74**, 283295 (2017).
- [13] T. Odenthal, B. Smeets, P. V. Liedekerke, E. Tijskens, H. V. Oosterwyck, and H. Ramon, “Analysis of initial cell spreading using mechanistic contact formulations for a deformable cell model,” *PLOS Computational Biology* **9**, e1003267 (2013).
- [14] J. L. McGrath, “Dispatch: Cell spreading: The power to simplify,” *Current Biology* **17**, R358 (2007).
- [15] Barnhart EL, Lee K-C, Keren K, Mogilner A, and Theriot JA, “An adhesion–dependent switch between mechanisms that determine motile cell shape,” *PLoS Biol* **9(5)** (2011).
- [16] P. K. Mattila and P. Lappalainen, “Filopodia: molecular architecture and cellular functions,” *Nature Publishing Group* **9** (2008).
- [17] M. Abu Hamed and A.A. Nepomnyashchya, “A simple model of keratocyte membrane dynamics: The case of motionless living cell,” *Physica D* **408** (2020).
- [18] M. Abu Hamed and A.A. Nepomnyashchya, “Dynamics of curved fronts in systems with power-law memory,” *Physica D* **328–329**, 1–8 (2016).
- [19] M. Abu Hamed and A.A. Nepomnyashchya, “Three–dimensional phase field model for actin–based cell membrane dynamics,” submitted to *The European Journal of Applied Mathematics* (2021).